Title: Quantification and visualization of the tumor microenvironment heterogeneity from spatial transcriptomic experiments

Oscar E. Ospina[1], Christopher M. Wilson[1], Alex C. Soupir[1], Anders Berglund[1], Inna Smalley[2], Kenneth Y. Tsai[2,3], and Brooke L. Fridley[1*]

[1] Department of Biostatistics and Bioinformatics, Moffitt Cancer Center, Tampa, FL, USA
[2] Department of Tumor Biology, Moffitt Cancer Center, Tampa, FL, USA
[2] Department of Anatomic Pathology, Moffitt Cancer Center, Tampa, FL, USA

Running title: Tumor heterogeneity using spatial transcriptomics

Keywords: Spatial array, tumor microenvironment, spatial heterogeneity, RNA-Seq, spatial kriging, unsupervised clustering

Financial support: This work was supported by the NIH – H. Lee Moffitt Cancer Center T32 Integrated Program in Cancer and Data Science (T32CA233399), and the Biostatistics and Bioinformatics Shared Resource at the H. Lee Moffitt Cancer Center and Research Institute, an NCI designated Comprehensive Cancer Center (P30-CA076292). IS is supported by the NIH R00 CA226679. This content is solely the responsibility of the authors and does not necessarily represent the official view of the NIH.

*Correspondence:
Brooke L. Fridley, Ph.D.
12902 Magnolia Drive
Moffitt Cancer Center
Tampa, FL 33612
Phone: 813-745-1461
Fax: 813-745-6107
Email: brooke.fridley@moffitt.org

Conflicts of interests: None of the authors have conflict-of-interest or financial disclosures to declare.

Word count: 1692 (from Introduction to Discussion)

Tables and figures: five figures (two in main text, four in supplementary information); one supplementary table.

Abstract

Spatially-resolved transcriptomic technologies promise to increase our understanding of the tumor microenvironment, which will lead to better cancer prognosis and therapies. Several spatial transcriptomics technologies have been developed, as well as a few methods for data analysis. Nonetheless, analytical pipelines that take users from gene counts to association of tumor spatial heterogeneity with clinical data are not available. Here we present spatialGE, a software that provides visualizations and quantification of the tumor microenvironment heterogeneity using spatial transcriptomics. Our software includes: 1) generation of high-resolution gene expression surfaces via spatial interpolation; 2) quantification of spatial heterogeneity measures that can be compared against clinical information (e.g., patient survival); 3) cell deconvolution methods at the spot level; 4) spatially-informed clustering; and 5) a new data structure that allows storage and analysis of multiple ST samples simultaneously. We show the utility of spatialGE by studying the spatial heterogeneity of cutaneous malignant melanoma samples.

Significance: spatialGE enables the analysis of spatial transcriptomics samples and exploration of the tumor microenvironment, as well as the association of clinical outcomes with the spatial variation in gene expression.

61 # Introduction

62 Spatially-resolved transcriptomic (ST) methods have allowed a better understanding of
63 the tumor microenvironment (TME) at an unprecedented resolution (1). Characterizing
64 heterogeneity within the TME is key to cancer prognosis and development of therapies (2,3).
65 Advances in ST promise to unravel tumor heterogeneity at different scales, from gene expression
66 differences among samples to clonal diversity within tissues (4). Importantly, the study of the
67 TME is crucial to comprehend immune infiltration and the relationship with immunotherapy
68 response (5).

69 Several ST technologies to study the TME have been developed (6-12). The most
70 common approach involves mRNA probe hybridization in immobilized tissues on surfaces (7).
71 These technologies can produce data for either a subset of genes (e.g., panel) or the whole
72 transcriptome (7). Spatial transcriptomics preserves the localization of gene expression within
73 the tissue architecture (13), as opposed to bulk RNA (RNA-seq) or in single-cell RNA
74 sequencing (scRNAseq) where tissue homogenization or dissociation is necessary (14).
75 Therefore, besides the high dimensionality of RNA-seq, the analysis needs to account for the
76 spatial location of transcripts. Consequently, data structures are needed to accommodate both
77 expression and spatial data, as well as related information (e.g., clinical information,
78 demographics). Similarly, methods for the visualization and analysis of tissue spatial
79 heterogeneity are needed, with existing tools varying in flexibility and approaches (15-20).
80 Hence, we developed spatialGE, a pipeline for the processing and analysis of ST experiments.
81 The pipeline borrows ideas from geostatistical techniques and applies them to the exploration of
82 the TME. The novel features of spatialGE include: 1) generation of transcriptomic surfaces; 2)
83 quantification of gene expression spatial heterogeneity and association with clinical information;

3) immune gene expression deconvolution methods; 4) spatially-informed clustering; and 5) a data structure to store gene counts, spatial, and sample metadata for multiple ST tissue sections.

Materials and Methods

Spatial transcriptomics data input and transformation

In spatialGE, for each tissue section the user provides count data, with gene names following the HUGO nomenclature. Spot coordinates should also be provided per tissue section. Optionally, an additional, single table can be provided containing associated clinical variables (Fig. 1A). The example data set presented with the spatialGE software is the Thrane et al. study of cutaneous malignant melanoma (21). The spatialGE software processes raw counts with library size normalization (22) followed by voom transformation (23) to produce roughly Gaussian distributed gene expression values per gene (Supplementary Figure 1). Relative gene expression at each spot can then be visualized using "quilt plots" (Fig. 1B).

Spatial transcriptomic surfaces estimation via interpolation ("kriging")

Visualization of spatial patterns in gene expression within the TME can be improved with the generation of transcriptomic surfaces. To produce smooth transcriptomic surfaces, spatialGE uses spatial interpolation (24) with either ordinary and universal kriging used to predict surfaces based on gene expression values or deconvoluted cell type scores (Fig. 1B-C). Ordinary kriging assumes a constant mean value across the sampled area (stationarity). Conversely, universal kriging assumes the mean gene expression varies across the tissue (24).

Spatial transcriptomics heterogeneity statistics

107 In addition to ST surfaces, spatialGE provides users with approaches to quantify spatial
108 heterogeneity across and detection of "hot-spots". A variety of measures are included to provide
109 a summary of TME heterogeneity (Supplementary Table XXSP_STATS; Fig. 1B): Moran's I
110 (25) and Geary's C (26) allow users to ascertain whether gene expression is uniform or
111 concentrated in specific tissue regions. The Getis-Ord G_i statistic measures the tendency of a
112 given gene to produce areas of concentrated high expression (hot-spots) or low expression (cold-
113 spots) (27). The use of spatial statistics allows to quantify associations with other measurable
114 variables from clinical outcomes. The statistics were implemented using the R package spdep
115 (28).
116
117 **Spatial transcriptomics gene expression deconvolution**
118 For cell type deconvolution, xCell (29) has been implemented to infer cell compositions
119 at each spot. Kriging can then be applied to these scores to obtain a spatial surface for a given
120 cell type (Fig.1C). Additionally, tumor purity scores are generated using ESTIMATE (30),
121 followed by classification of spots as primarily tumor or stroma using Gaussian model-based
122 clustering, as implemented in the R package mclust (31).
123
124 **Unsupervised spatially-informed clustering to infer TME expression subtypes**
125 To understand the location and types of different TME compartments, unsupervised
126 spatially-informed clustering can be performed (Fig. 1D). For clustering, principal component
127 analysis (PCA) of gene counts is completed. Then, a spatially-informed distance matrix for
128 clustering is computed based on two scaled distance matrices: 1) transcriptomic autocorrelation
129 between spots using the principal components (D_1), and 2) spatial distances between spots (D_2).

130 Next, the autocorrelation matrix is "shrunk" toward the physical distance matrix by calculating a
131 weighted average distance matrix:

132 $$D = [(1 - w) * D_1] + (w * D_2)$$

133 The user specifies the weight (w) to apply. Based on our experience a weight between
134 0.05 and 0.25 seems to best capture tissue heterogeneity, without too much "shrinkage". Using
135 the weighted matrix, *D*, hierarchical clustering with dynamic cut-points (32) can be completed to
136 derive the TME compartments, without the need to specify the number of compartments.
137

138 **Availability**

139 spatialGE is available as an R package at https://github.com/FridleyLab/spatialGE. A
140 tutorial is also provided showing users how to use the package and its various features. A script
141 to reproduce the analyses in this manuscript is available in Supplementary Information.
142

143 Results

144 The utility of spatialGE is demonstrated using the Thrane et al. ST tissue sections, with
145 equidistant spots of 100μM diameter and 200μM apart (21). The eight tissue sections
146 (representing four patients) had an average of 15,864 genes, and average number of spots of 293
147 (range = 212–383). Both quilt plots and transcriptomic surfaces of genes relevant to cutaneous
148 malignant melanoma captured the heterogeneity of the tumor and stromal compartments (Fig.
149 2A, Supplementary Fig. 2), consistent with pathology images in the Thrane et al. study (21).
150 With spatialGE, we could also reproduce their findings on the spatial patterns of gene
151 expression. For example, in tissue section 2 (patient 1), the genes *PMEL* and *SPP1* were
152 expressed throughout the tissue, except in a region classified as lymphoid tissue (Supplementary

153 Fig. 2A-B). Conversely, *CD74* and *IGLL5* exhibited the opposite pattern, with low expression in
154 the melanoma region (Fig. 2A, Supplementary Fig. 2C-D). The expression of *SOX10* was high
155 across the tissue section, whereas SOX4 expression was low in spots classified as tumor by the
156 ESTIMATE scores (Supplementary Fig. 2E-F). Future research could study the potential use of
157 *SOX4* to identify melanoma regions using data from ST experiments.

158 The spatial autocorrelation statistics (Moran's I, Geary's C, and Getis-Ord G_i) captured
159 gene expression heterogeneity across the tissue and showed moderately strong relationships with
160 standard deviation ($0.49 < R^2 < 0.64$; Fig. 2B). A higher degree of spatial heterogeneity was
161 found for *CD74* compared to *SOX10*, as indicated by Moran's I (I=0.20 and I=0.02,
162 respectively). Nonetheless, *SOX10* showed higher Geary's C (Supplementary Fig. 2D-E),
163 reflecting Geary's C higher sensitivity to smaller agglomerations of high expression. The Getis-
164 Ord G_i statistic, a measure of "hot-spots", indicated that expression of *PMEL* and *SPP1* had a
165 strong tendency to generate high expression regions (Supplementary Fig. 2A-B). Interestingly,
166 Moran's I and Geary's C calculated for *CD74* showed an association between spatial
167 heterogeneity in the biopsies and patient survival, with >120 months survival observed when
168 *CD74* exhibited high spatial association (Fig. 2C).

169 After immune cell deconvolution for each spot, kriging of B cell scores showed a
170 transition from high scores in stroma to low scores nearing the melanoma compartment. This
171 finding was congruent with ESTIMATE binary tumor/stroma classifications (patient 1; Fig. 2A).
172 Spatially-informed clustering with $w = 0.075$ seemed to capture the tissue heterogeneity of the
173 tumor when compared to the pathology images in Thrane et al. (21) (Supplementary Fig. 3 and.
174 4). The first and second clusters corresponded to melanoma and stromal areas. The third cluster

175 surrounded the melanoma area and included spots in the region of high B cell scores (Fig. 2D;
176 Supplementary Fig. 3).
177

178 # Discussion

179 Our pipeline, spatialGE, provides visualizations of spatially-resolved gene expression, as
180 well as quantification of TME heterogeneity and exploration of its potential associations with
181 clinical information. Gene expression visualizations at high resolution are offered by few tools
182 (20), however spatialGE is unique in implementing kriging to achieve this task for multiple ST
183 tissue sections simultaneously. Unlike other approaches, kriging gives users flexibility to choose
184 visualization resolution with few modeling assumptions. Additionally, kriging is used to
185 visualize tissue composition as inferred by deconvolution methods. Our pipeline also features
186 unsupervised spatially-informed clustering, a simple yet informative method to detect TME
187 compartments. Several ST clustering approaches are already available (16-18,20), however our
188 method resembles tissue features by weighting transcriptomic similarities between spots by their
189 distances to one another. Another innovation of spatialGE is the estimation of quantifiable
190 metrics (spatial heterogeneity statistics) to capture transcriptomic complexity and the ability to
191 compare them against patient clinical outcomes. A comparison between spatialGE and other
192 software is available in the supplementary information (Supplementary Table 2).
193 Applying spatialGE to the melanoma ST data, we observed agreement between the
194 transcriptomic surfaces and the tumor and stroma regions observed in pathology images (21).
195 Our spatially-informed clustering approach provided TME compartments (i.e., clusters) that
196 resembled the features annotated in pathology images (21), with an immune tumor border effect
197 observed, in which the melanoma compartments were surrounded by regions with high B cell

198 scores. Finally, we observed an association between spatial heterogeneity and clinical variables
199 providing support to the hypothesis that spatial heterogeneity is a predictor of patient outcomes
200 (3). For example, higher levels of *CD74* (indicated by Moran's I and Geary's C) corresponded to
201 longer survival.

202 In future spatialGE versions, we will include features to analyze a wider ST technology
203 spectrum. We are currently developing gene expression visualizations and histological
204 annotation of spots for technologies using non-gridded arrangements, as well as a web-based
205 implementation of spatialGE. Another developing area is the integration of scRNA-seq data to
206 provide ST cell-level insights. Finally, we are expanding our spatially-informed clustering
207 method to identify genes that differ among clusters.

208 In summary, spatialGE provides a suite of methods for the exploration of the TME via
209 ST. By adapting geostatistical methods (e.g., kriging and autocorrelation statistics) and a novel
210 spatially-informed clustering, we provided an innovative approach to the study processes such as
211 immune infiltration and the effect of TME architecture on patient outcomes.

212

213 Disclosure of Potential Conflicts of Interest

214 No potential conflicts of interest were disclosed.

215

216 Acknowledgments

217 We thank the spatial research group at the KTH Royal Institute of Technology – SciLifeLab
218 (Stockholm, Sweden) for making their melanoma data available.

219

220 References

221 1. Moor AE, Itzkovitz S. Spatial transcriptomics: paving the way for tissue-level systems
222 biology. Curr Opin Biotechnol **2017**;46:126-33
223 2. Marusyk A, Almendro V, Polyak K. Intra-tumour heterogeneity: a looking glass for
224 cancer? Nat Rev Cancer **2012**;12:323-34
225 3. Nederlof I, Horlings HM, Curtis C, Kok M. A High-Dimensional Window into the
226 Micro-Environment of Triple Negative Breast Cancer. Cancers (Basel) **2021**;13
227 4. Saviano A, Henderson NC, Baumert TF. Single-cell genomics and spatial
228 transcriptomics: Discovery of novel cell states and cellular interactions in liver
229 physiology and disease biology. J Hepatol **2020**;73:1219-30
230 5. Tang H, Qiao J, Fu YX. Immunotherapy and tumor microenvironment. Cancer Lett
231 **2016**;370:85-90
232 6. Stahl PL, Salmen F, Vickovic S, Lundmark A, Navarro JF, Magnusson J*, et al.*
233 Visualization and analysis of gene expression in tissue sections by spatial
234 transcriptomics. Science **2016**;353:78-82
235 7. Zhang M, Sheffield T, Zhan X, Li Q, Yang DM, Wang Y*, et al.* Spatial molecular
236 profiling: platforms, applications and analysis tools. Brief Bioinform **2021**;22
237 8. Xia C, Fan J, Emanuel G, Hao J, Zhuang X. Spatial transcriptome profiling by MERFISH
238 reveals subcellular RNA compartmentalization and cell cycle-dependent gene expression.
239 Proc Natl Acad Sci U S A **2019**;116:19490-9
240 9. Merritt CR, Ong GT, Church SE, Barker K, Danaher P, Geiss G*, et al.* Multiplex digital
241 spatial profiling of proteins and RNA in fixed tissue. Nat Biotechnol **2020**;38:586-99

242 10. Wang X, Allen WE, Wright MA, Sylwestrak EL, Samusik N, Vesuna S*, et al.* Three-
243 dimensional intact-tissue sequencing of single-cell transcriptional states. Science
244 **2018**;361
245 11. Vickovic S, Eraslan G, Salmen F, Klughammer J, Stenbeck L, Schapiro D*, et al.* High-
246 definition spatial transcriptomics for in situ tissue profiling. Nat Methods **2019**;16:987-90
247 12. Rodriques SG, Stickels RR, Goeva A, Martin CA, Murray E, Vanderburg CR*, et al.*
248 Slide-seq: A scalable technology for measuring genome-wide expression at high spatial
249 resolution. Science **2019**;363:1463-7
250 13. Maniatis S, Petrescu J, Phatnani H. Spatially resolved transcriptomics and its applications
251 in cancer. Curr Opin Genet Dev **2021**;66:70-7
252 14. Yu X, Abbas-Aghababazadeh F, Chen YA, Fridley BL. Statistical and Bioinformatics
253 Analysis of Data from Bulk and Single-Cell RNA Sequencing Experiments. Methods
254 Mol Biol **2021**;2194:143-75
255 15. Navarro JF, Sjostrand J, Salmen F, Lundeberg J, Stahl PL. ST Pipeline: an automated
256 pipeline for spatial mapping of unique transcripts. Bioinformatics **2017**;33:2591-3
257 16. Bergenstrahle J, Larsson L, Lundeberg J. Seamless integration of image and molecular
258 analysis for spatial transcriptomics workflows. BMC Genomics **2020**;21:482
259 17. Tan X, Su A, Tran M, Nguyen Q. SpaCell: integrating tissue morphology and spatial
260 gene expression to predict disease cells. Bioinformatics **2020**;36:2293-4
261 18. Dries R, Zhu Q, Dong R, Eng CL, Li H, Liu K*, et al.* Giotto: a toolbox for integrative
262 analysis and visualization of spatial expression data. Genome Biol **2021**;22:78
263 19. Sun S, Zhu J, Zhou X. Statistical analysis of spatial expression patterns for spatially
264 resolved transcriptomic studies. Nat Methods **2020**;17:193-200

265 20. Zhao E, Stone MR, Ren X, Guenthoer J, Smythe KS, Pulliam T*, et al.* Spatial
266 transcriptomics at subspot resolution with BayesSpace. Nat Biotechnol **2021**
267 21. Thrane K, Eriksson H, Maaskola J, Hansson J, Lundeberg J. Spatially Resolved
268 Transcriptomics Enables Dissection of Genetic Heterogeneity in Stage III Cutaneous
269 Malignant Melanoma. Cancer Res **2018**;78:5970-9
270 22. Robinson MD, McCarthy DJ, Smyth GK. edgeR: a Bioconductor package for differential
271 expression analysis of digital gene expression data. Bioinformatics **2010**;26:139-40
272 23. Law CW, Chen Y, Shi W, Smyth GK. voom: Precision weights unlock linear model
273 analysis tools for RNA-seq read counts. Genome Biol **2014**;15:R29
274 24. Diggle PJ, Ribeiro PJ. Spatial prediction. Model-based Geostatistics. New York, NY:
275 Springer New York; 2007. p 134-56.
276 25. Moran PA. Notes on continuous stochastic phenomena. Biometrika **1950**;37:17-23
277 26. Geary RC. The contiguity ratio and statistical mapping. The incorporated statistician
278 **1954**;5:115-46
279 27. Getis A, Ord JK. The analysis of spatial association by use of distance statistics.
280 Perspectives on spatial data analysis: Springer; 2010. p 127-45.
281 28. Bivand R, Anselin L, Berke O, Bernat A, Carvalho M, Chun Y*, et al.* spdep: Spatial
282 dependence: weighting schemes, statistics and models: R package version 0.5-31, URL
283 http://CRAN. R-project. org/package= spdep; 2011.
284 29. Aran D, Hu Z, Butte AJ. xCell: digitally portraying the tissue cellular heterogeneity
285 landscape. Genome Biol **2017**;18:220

286 30. Yoshihara K, Shahmoradgoli M, Martinez E, Vegesna R, Kim H, Torres-Garcia W*, et al.*
287 Inferring tumour purity and stromal and immune cell admixture from expression data.
288 Nat Commun **2013**;4:2612
289 31. Scrucca L, Fop M, Murphy TB, Raftery AE. mclust 5: Clustering, Classification and
290 Density Estimation Using Gaussian Finite Mixture Models. R Journal **2016**;8:289-317
291 32. Langfelder P, Zhang B, Horvath S. Defining clusters from a hierarchical cluster tree: the
292 Dynamic Tree Cut package for R. Bioinformatics **2008**;24:719-20
293

294 # Figure captions

295 **Figure 1.** Inputs (A) and outputs (B-D) from the analysis of spatially resolved transcriptomic
296 data using spatialGE. **A.** Gene count matrices (*M*) with features (*g*) as rows and spots (*s*) as
297 columns, as well as spot coordinates (*C*) are used to create a Spatial Transcriptomics List
298 (STList). Optionally, a table with data on clinical variables (*V*) can be provided. **B.** Gene counts
299 are voom-transformed, and "quilt" plots can be generated showing expression of a given gene at
300 each spot. The transformed expression values can also be used to generate transcriptomic
301 surfaces via "kriging". Spatial autocorrelation statistics are also calculated (e.g., Moran's I),
302 which can be used to explore their relationship with clinical information (e.g., survival). **C.** Gene
303 expression deconvolution via xCell and ESTIMATE is performed and immune cell type surfaces
304 can be plotted, as well as classifications of spots into tumor or stroma compartments. **D.**
305 spatialGE implements hierarchical clustering of the spots by weighting the transcriptomic
306 differences in gene expression with the spatial distances between spots.
307

308 **Figure 2.** Results from spatialGE analysis of a melanoma stage IIIc using spatial transcriptomics
309 (patient 1, slice 2 (21)). **A.** Quilt plot showing voom-transfromed expression at each spot for
310 immune gene *CD74*, with squares and crosses indicating tumor and stromal spots respectively, as
311 inferred by ESTIMATE (A–top left). The tumor and stromal assignments can also be observed
312 also in the accompanying plot (A–top right). A transcriptomic surface of *CD74* expression
313 allows for a clearer visualization of the tissue heterogeneity (A–bottom left), with gray squares
314 indicating the ESTIMATE tumor assignments. The inferred abundance of B cells in the tissue
315 can be visualized by the predicted surface of xCell scores (A–bottom right). **B.** Relationship
316 between the spatial autocorrelation statistics and standard deviation of gene expression. The red

317 dot represents *CD74*, and asterisk (*) indicates a significant relationship between the spatial
318 statistic and the standard deviation. **C.** Scatter plots showing the relationships between spatial
319 statistics calculated for *CD74* and the survival of patients in months (21). The colored arrows
320 provide a guide for the interpretation of the spatial statistics. The dot with black border indicates
321 the tissue section from patient 1 featured in panels the rest of the panels. **D.** ESTIMATE
322 tumor/stroma assignments and spatially-informed clusters (using a spatial weight of 0.1) are
323 shown. The yellow (1) and blue (2) clusters roughly represent tumor and stroma spots
324 respectively. The red cluster (3) likely correspond to spots showing immune activity given the
325 topological match with B cell scores (see **A**).
326
327

328 # Supplementary Figure captions

329 **Supplementary Fig. 1.** Raw and voom-transformed counts for a set of genes within the
330 melanoma ST array 1 from patient 1 (21): **A.** *PMEL*; **B.** *SPP1*; **C.** *SOX10*; **D.** *CD74*.
331

332 **Supplementary Fig. 2.** Transcriptomic surfaces resulting from spatial interpolation ("kriging")
333 of *PMEL* (**A**), *SPP1* (**B**), *CD74* (**C**), *IGLL5* (**D**), *SOX10* (**E**), and *SOX4* (**F**). The same genes are
334 shown for all the tissue slices in Thrane et al. (21).
335

336 **Supplementary Fig. 3.** Cluster assignment of the spots as generated by unsupervised spatially-
337 informed clustering and dynamic tree cuts. Spatial weights (w) from 0.0 to 0.5 were evaluated.
338 **A.** w=0; **B.** w=0.025; **C.** w=0.05; **D.** w=0.0.75; **E.** w=0.1; **F.** w=0.15; **G.** w=0.2; **H.** w=0.5.
339

340 **Supplementary Fig. 4.** Cluster assignment of the spots as generated by unsupervised spatially-
341 informed clustering and different values of k from 2 to 5. **A.** k=2; **B.** k=3; **C.** k=4; **D.** k=5. Each
342 page in this file shows clusters at different spatial weights from w=0.0 to w=0.5.
343

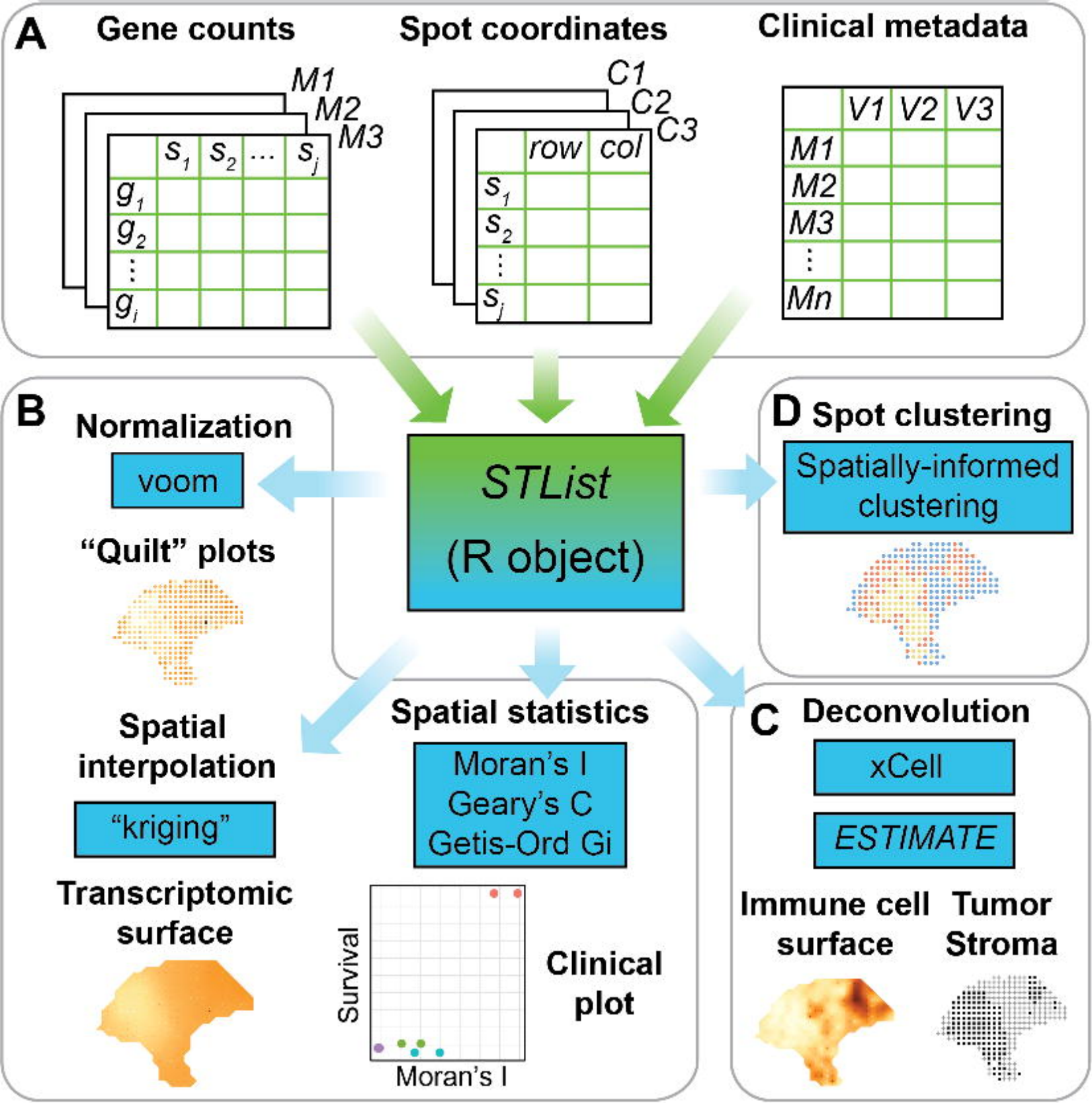
A
Gene counts
M1
M2
M3
s1 s2 … sj
g1
g2
gi
Spot coordinates
C1
C2
C3
row col
s1
s2
sj
Clinical metadata
V1 V2 V3
M1
M2
M3
Mn
STList
(R object)
B
Normalization
voom
"Quilt" plots
Spatial interpolation
"kriging"
Transcriptomic surface
Spatial statistics
Moran's I
Geary's C
Getis-Ord Gi
Survival
Moran's I
Clinical plot
D Spot clustering
Spatially-informed clustering
C Deconvolution
xCell
ESTIMATE
Immune cell surface
Tumor Stroma

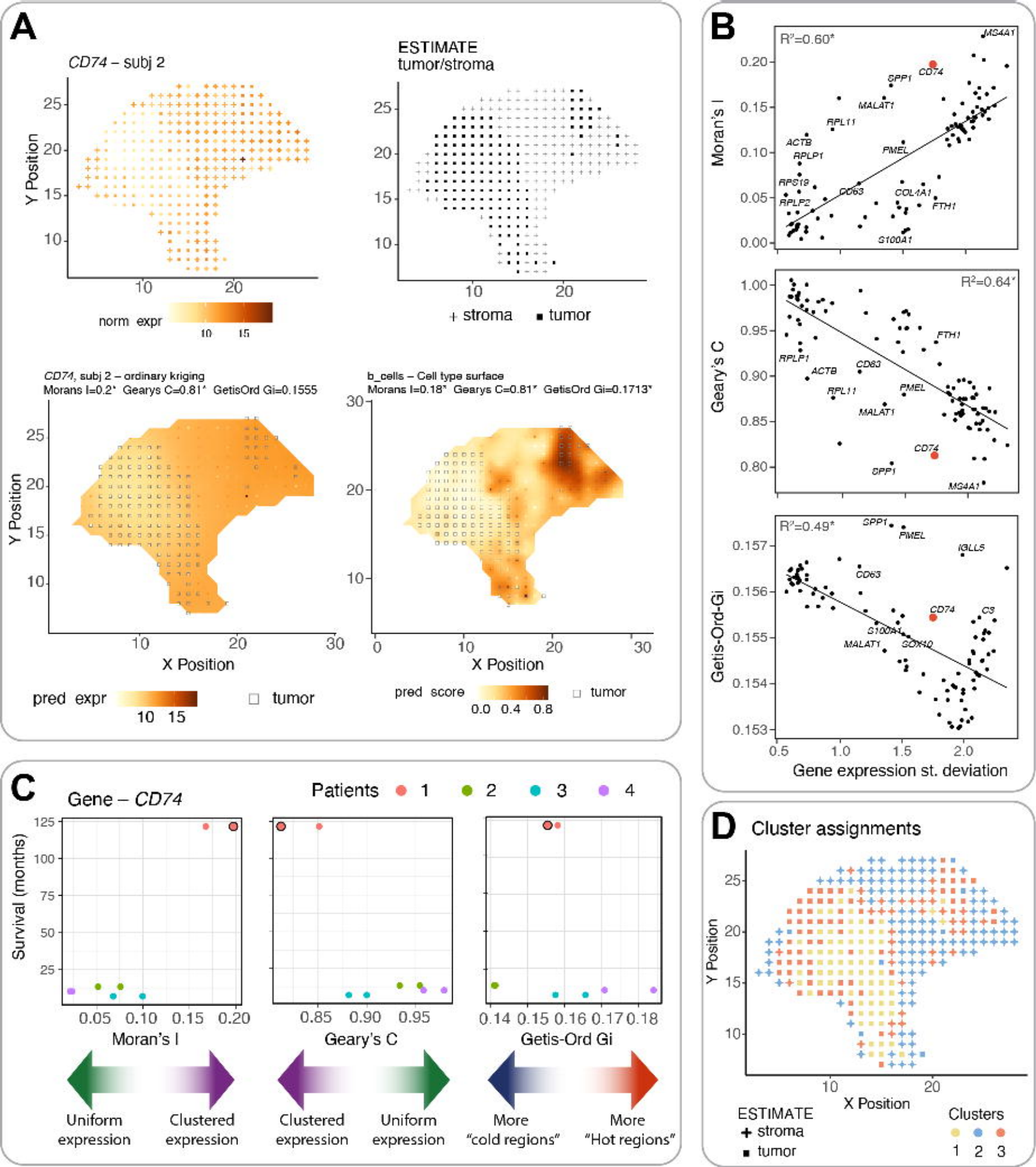
A
CD74 – subj 2
Y Position
norm expr
ESTIMATE
tumor/stroma
stroma
tumor
CD74, subj 2 – ordinary kriging
Morans I=0.2* Gearys C=0.81* GetisOrd Gi=0.1555
X Position
pred expr
tumor
b_cells – Cell type surface
Morans I=0.18* Gearys C=0.81* GetisOrd Gi=0.1713*
pred score
B
R²=0.60*
Moran's I
R²=0.64*
Geary's C
R²=0.49*
Getis-Ord-Gi
Gene expression st. deviation
C
Gene – CD74
Patients 1 2 3 4
Survival (months)
Moran's I
Geary's C
Getis-Ord Gi
Uniform expression
Clustered expression
Clustered expression
Uniform expression
More "cold regions"
More "Hot regions"
D
Cluster assignments
Y Position
X Position
ESTIMATE
stroma
tumor
Clusters
1 2 3